JOURNAL OF CATALYSIS 97, 100–107 (1986)

Oxidation of Carbon Monoxide on Thin Film Catalysts: Characterization in a Large Range of Pressure by Detection of a Transition between Stationary States

J.-P. DATH[1] AND J. P. DAUCHOT

Université de l'Etat à Mons, Faculté des Sciences, Service de Chimie Analytique et Inorganique, Avenue Maistriau 23, 7000 Mons, Belgium

Received March 14, 1984; revised March 18, 1985

Carbon monoxide oxidation has been studied in a large range of pressures (from 5×10^{-3} to 100 Torr) over thin polycrystalline and epitaxial (100) platinum films. The transition between two stationary states characterizing this reaction has been detected by using a Kelvin probe. On polycrystalline films, the study is considerably limited by recrystallization but the epitaxial films are very stable. Some results indicate that the catalyst surface is contaminated in some conditions. Nevertheless, kinetic parameters are tentatively calculated and are found to be in good agreement with the literature values.

1. INTRODUCTION

Carbon monoxide oxidation over platinum is of great interest in the fundamental study of surface reactions. This reaction presents a transition between two stationary states. The critical temperature, which is defined as the transition temperature, has been measured at atmospheric pressure on polycrystalline platinum thin films. It appears that measurement of the critical temperature is a very sensitive method for characterization of the catalyst (*1*).

We examine here the transition in a large range of pressures (from 5×10^{-3} to 100 Torr) not only on polycrystalline films but also on epitaxial Pt(100) films.

Due to the lower surface/volume ratio of the well-oriented films, it was no longer possible to use an electrical resistance measurement for detecting the transition. Instead, measurement of the surface potential by the Kelvin method was chosen. Indeed, it was shown earlier (*2*) that the transition between the two stationary states is accompanied by a large surface potential variation which may be explained by a dramatic change of CO and oxygen coverage (*3*).

2. EXPERIMENTAL

The work function change is measured using the vibrating capacitor built by Delta-Phi Elektronik, Jülich. The experiments are performed in a turbomolecular pumped high vacuum (HV) system. As in our previous work (*1*), all the measurements are made in dynamic conditions. The catalyst surface is very small (5 mm × 5 mm) compared to the reactor volume, the pumping rate is very high, and all the gas in the reactor cell is renewed in less than 10 sec. Therefore the conversion factor remains low. The carbon monoxide and oxygen flows are regulated by a couple of flowmeters (Brooks thermal flowmeters) and are introduced at atmospheric pressure into the core of a leak-valve by which the pressure in the reactor cell is fixed with good accuracy. The gas flow in excess passes through another flowmeter which allows us to check that the total flow is always in surplus.

The sample is fixed on a thermostabilized gold-plated copper block. The position of the probe can be adjusted over the specimen (Fig. 1). The pressure is measured by a Balzers H.P. gauge (from 5×10^{-3} to 2×10^{-1} Torr) or by a membrane gauge (100 Torr). Instead of measuring the critical tem-

---

[1] IRSIA specialization fellowship.

0021-9517/86 $3.00

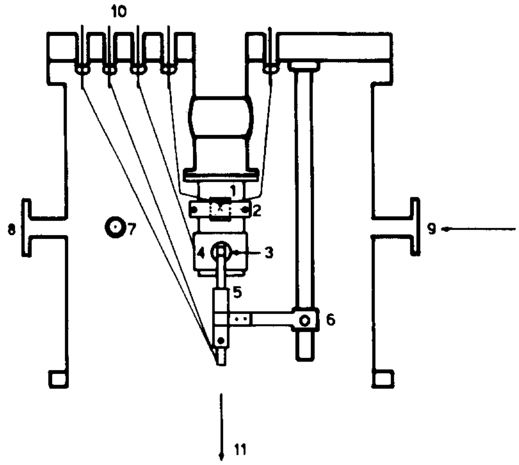

FIG. 1. Experimental setup: 1, thermostabilized gold-plated copper block; 2, thermocouple; 3, sample; 4, sample holder; 5, Kelvin probe; 6, Kelvin probe support; 7, Balzers H.P. ionization gauge; 8, membrane gauge; 9, gas inlet via a leak valve; 10, electrical feedthroughs; 11, to the turbomolecular pump.

perature as before (*1*), we have measured the critical carbon monoxide concentration by decreasing progressively the CO concentration and following on a recorder the change of contact potential difference between the sample and the gold-plated Kelvin probe. The transition is detected from the inhibited to the active phase in order that the transition is not affected by reaction heat dissipation and carbon monoxide diffusion [these two points were discussed in the previous paper (*1*)]. The temperature is measured by a thermocouple pressed against the copper block.

Between all the measurements, the samples are heated in pure CO at the temperature and the pressure of the preceding transition.

The epitaxial Pt(100) films are synthesized on LiF(100) in ultrahigh vacuum (UHV) conditions following an experimental procedure which is described later. The polycrystalline Pt films are prepared by PtO_2 decomposition (*1*).

3. RESULTS

On the two types of platinum thin films (decomposed PtO_2 or epitaxial Pt(100)), the critical [CO]/[O_2] ratio is greater than at atmospheric pressure. This is in good agreement with the results obtained in UHV. (*4*, *5*).

On the other hand, on the epitaxial samples, a temperature limit below which the transition can no longer be detected by the Kelvin probe has been observed. This temperature limit rises as the total pressure decreases.

Another point to be noted is an important change of the contact potential difference appearing in the inhibited phase as soon as a very low oxygen partial pressure is introduced in the reactor cell. It cannot be confused with the transition, this latter being detected at a lower [CO]/[O_2] ratio and followed by oscillations.

Study of the Critical CO Concentration Versus Temperature

On epitaxial Pt(100) film. In Fig. 2a, the logarithm of the critical [CO]/[O_2] ratio is plotted versus $1/T$. Due to the small range of temperatures and the imprecision of the measurements, a straight line fit is used. This does not prove necessarily that the law is linear.

The straight lines differ with the total pressure. The slopes and the ordinate axis intercepts are reproduced in Table 1 and plotted versus the logarithm of the total pressure in Figs. 3a and 3b.

On polycrystalline Pt films. This type of sample is prepared as PtO_2 deposited on oxidized silicon wafers by d.c. reactive sputtering in an oxygen–argon mixture. They are stored in this form and decomposed to platinum just before the experiments (*1*).

The results are reproduced in Fig. 2b. It must be noted that this type of platinum film undergoes a large alteration during the measurements despite the intermediate treatment described above. The main cause of this behavior is probably recrystallization (*1*).

At lower pressures than 5×10^{-2} Torr, the results are quite incoherent.

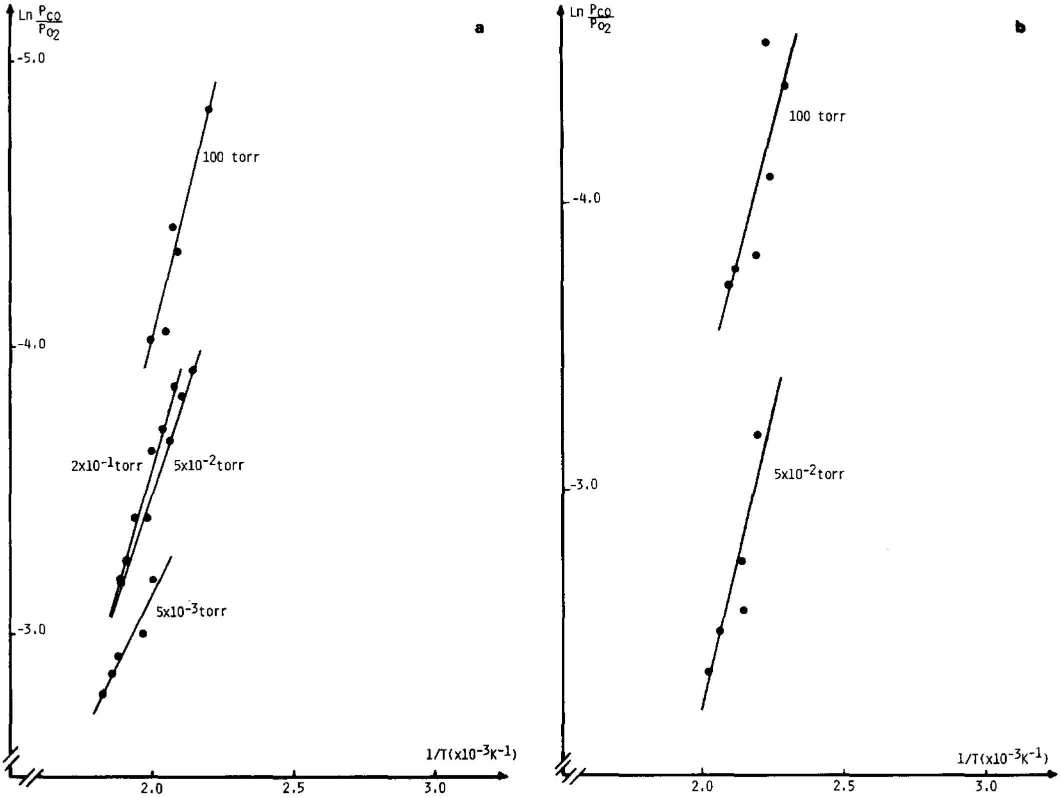

FIG. 2. "Arrhenius" plot of the critical [CO]/[O$_2$] ratios determined at constant temperature versus 1/T (a) on epitaxial Pt(100) film and (b) on polycrystalline Pt film.

TABLE 1

Kinetic Parameters Calculated at the Transition from Experimental Results Obtained on Epitaxial Pt(100) Film and from Equations (12) to (15), with N_S = 5 × 10^{18} sites/m^2

Total pressure (Torr)	$B_2'' \times R$ (kcal/mole)	X	B_1/B_2	σ_{CO}/σ_{O_2}[a]	B_2/C	σ_{O_2}/C'[a]
5×10^{-3}	1	0.21	0.58	3.97	0.13	3.13×10^{-11}
	2	0.16	0.67	1.77	0.06	9.49×10^{-11}
	4	[b]	[b]	[b]	[b]	[b]
5×10^{-2}	1	0.34	0.32	3.50	1.09	1.46×10^{-11}
	2	0.31	0.38	1.51	0.68	6.62×10^{-11}
	4	0.22	0.56	0.31	0.15	8.02×10^{-10}
2×10^{-1}	1	0.39	0.21	2.60	3.45	1.03×10^{-11}
	2	0.38	0.25	1.11	2.35	5.22×10^{-11}
	4	0.32	0.37	0.22	0.75	9.14×10^{-10}
100	1	0.48	0.04	1.05	130	4.09×10^{-13}
	2	0.48	0.05	0.44	90	2.30×10^{-12}
	4	0.46	0.07	0.08	39	6.51×10^{-11}

[a] For these calculated values the mean working temperature and the mean critical p_{CO}/p_{O_2} ratio have been considered.

[b] No physical value.

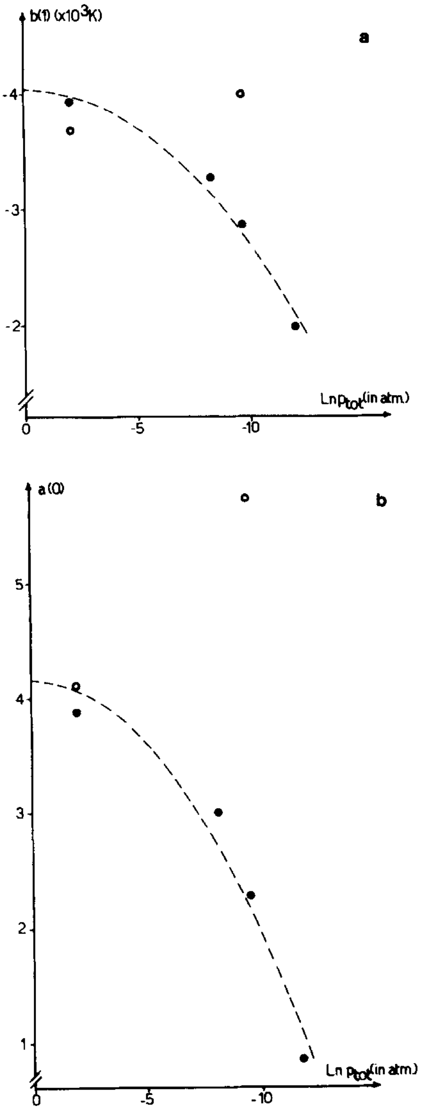

FIG. 3. (a) Figs. 2a (●) and 2b (○) ordinate axis intercepts plotted versus the logarithm of the total pressure. (b) Figs. 2a (●) and 2b (○) slopes plotted versus the logarithm of the total pressure.

4. DISCUSSION

a. Change of Surface Potential at Oxygen Introduction

The important change of contact potential when a low partial pressure of oxygen is introduced in the reactor cell could be explained by a preadsorption of oxygen. In his kinetic study, Winterbottom (*6*) showed that molecular oxygen interacts with the platinum surface before being dissociated and reacting with carbon monoxide. Moreover, not all the surface sites seem to promote the formation of atomic oxygen. However, it is generally assumed that the adsorbed oxygen is completely dissociated in the range of temperatures where this study has been made. Therefore it seems more realistic to consider this change of potential as being due to an oxygen interaction with impurities at the platinum surface (*3*).

b. Arrhenius Plot Interpretation

When considering the model of Dagonnier *et al.* (DDN) (*7*), it can be seen that the critical point [critical ratio [CO]/[O$_2$] at constant temperature or critical temperature at constant [CO]/[O$_2$] ratio is defined from the expression of carbon monoxide and atomic oxygen coverages (noted X and Y, respectively. When neglecting the Eley–Rideal contribution ($CO_{gas} + O_{ads} \rightarrow CO_2$) and the CO desorption ($CO_{ads} \rightarrow CO_{gas}$), Eqs. (14a) and (14b) of Ref. (*7*) are written as

$$\frac{dX}{dt} = B_1(1 - X - Y) - CXY \qquad (1)$$

$$\frac{dY}{dt} = B_2(1 - X - Y)^n - CXY$$

$$\text{with } n = 2 \text{ in our case,} \qquad (2)$$

where B_1, B_2, and C are, respectively, the rate constant of carbon monoxide adsorption, the dissociative oxygen adsorption, and the surface reaction. The thermal equation of Ref. (*7*) is not considered.

The steady states are reached when

$$\frac{dX}{dt} = 0 \quad \text{and} \quad \frac{dY}{dt} = 0, \qquad (3)$$

which gives

$$X \text{ or } Y = \frac{1}{2}\left(\frac{B_2 - B_1}{B_2}\right) \left[1 \pm \left(1 - \frac{4B_2/C}{\left(\frac{B_2}{B_1} - 1\right)^2}\right)^{1/2}\right], \qquad (4)$$

where B_1, B_2, and C are expressed as

$$B_1 = B_1' \exp(-B_1''/T)$$

$$\text{with } B_1' = \frac{\sigma_{CO} p_{CO}}{N_S \sqrt{2\pi m_{CO} kT}}$$

$$B_2 = B_2' \exp(-B_2''/T)$$

$$\text{with } B_2' = \frac{2\sigma_{O_2} p_{O_2}}{N_S \sqrt{2\pi m_{O_2} kT}}$$

$$C = C' \exp(-C''/T),$$

where m_{CO} and m_{O_2} are the molecular weights of each gas. N_S is defined as the number of active sites per unit area, σ_{CO} and σ_{O_2} are the sticking coefficients (exponential factor excluded), and k is the Boltzmann constant. C'', B_1'', B_2'' are the activation energies divided by the ideal gas constant R. The adsorbate is mixed when the solutions of Eq. (4) are real. Therefore, the critical point is obtained for a null discriminant:

$$1 - \frac{4B_2/C}{\left(\frac{B_2}{B_1} - 1\right)^2} = 0$$

$$\text{or } B_1/B_2 = (1 \pm 2\sqrt{B_2/C})^{-1} \qquad (6)$$

and at this point

$$X = Y = \tfrac{1}{2}(1 - B_1/B_2). \qquad (7)$$

Two limiting cases may be regarded. They appear as two distinct zones in Fig. 4 where the rate constant ratio B_2/C has been plotted versus the adsorption rate constant ratio B_1/B_2 at the transition.

The first case (zone A) where the rate constant of oxygen supply to the surface is greater than the surface reaction rate constant ($B_2 \gg C$) corresponds to the kinetic limited regime. The critical point is then defined by

$$B_1/B_2 = (2\sqrt{B_2/C})^{-1}, \qquad (8)$$

which is obtained by neglecting 1 in Eq. (6) (the minus sign is excluded since B_1/B_2 must be positive).

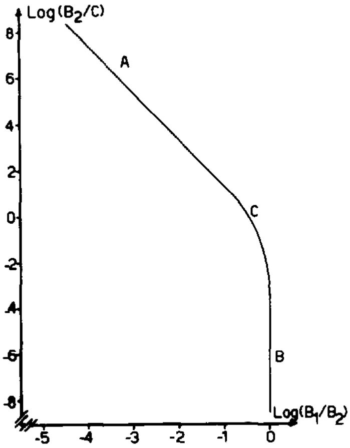

FIG. 4. Logarithm of the rate constant ratio B_2/C plotted versus the logarithm of the rate constant ratio B_1/B_2 at the transition.

By taking the natural logarithm and equating the different terms, it follows that [it is considered that $B_1'' = 0$ (*3*, *9*)]

$$2 \ln \frac{p_{CO}}{p_{O_2}} = -\frac{B_2'' + C''}{T} + \ln \left(\frac{C' \sigma_{O_2} N_S \sqrt{2\pi m_{O_2} kT}}{2 p_{O_2} \sigma_{CO}^2 \frac{m_{O_2}}{m_{CO}}} \right) \qquad (9)$$

or

$$\ln \frac{p_{CO}^2}{p_{O_2}} = -\frac{B_2'' + C''}{T} + \ln \left(\frac{C' \sigma_{O_2} N_S \sqrt{2\pi m_{O_2} kT}}{2 \sigma_{CO}^2 \frac{m_{O_2}}{m_{CO}}} \right). \qquad (10)$$

We have checked this latter relationship with our measurements in Figs. 5 and 6 (in Fig. 5, the $\sqrt{T}$ dependence is not taken into account and in Fig. 6 it is). Obviously the conditions leading to Eq. (10) are not fulfilled at low pressure. However, the aspect of Figs. 3a and 3b indicates that they belong to the high pressure regime as was assumed in our previous paper (*1*), since the slope and the ordinate axis intercept tend to the value obtained at atmospheric pressure as the total pressure increases.

Zone B of Fig. 4 corresponds to the diffu-

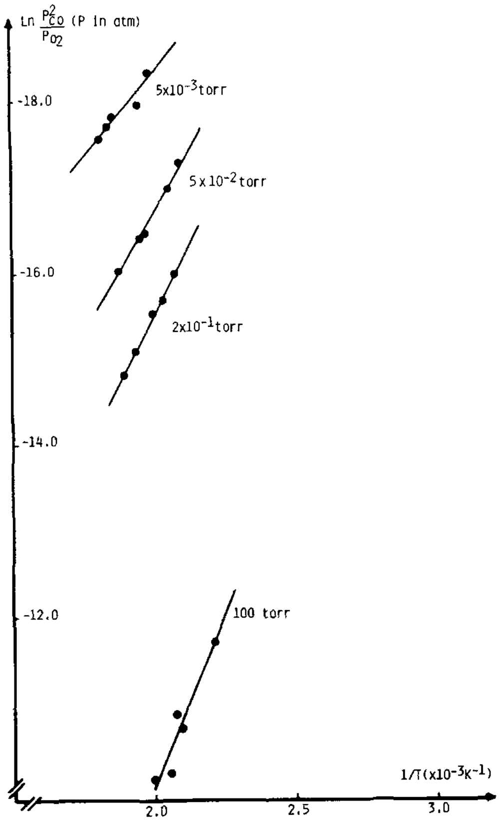

FIG. 5. Plot of the critical ln p^2_{CO}/p_{O_2} determined on epitaxial Pt(100) film versus $1/T$.

sion limited regime: the rate constant of oxygen supply to the surface is lower than the surface reaction rate constant ($B_2 \ll C$). If we put this condition in the coverage expression [Eq. (6)], it appears that the discriminant is zero for B_1/B_2 nearly equal to 1 and that the surface becomes bare at the transition. This could be correlated with the fact that the transition disappears at low pressure. However, it does not account for the temperature limit observed. Indeed the explicit Eq. (6) gives

$$\frac{B_1}{B_2} = \frac{1}{1 + 2\left(\frac{2\sigma_{O_2}p_{O_2}}{N_S C'\sqrt{2\pi m_{O_2}kT}}\right)^{1/2} \exp\left(-\frac{B_2'' - C''}{2T}\right)}. \quad (11)$$

Since $B_2'' - C''$ is negative (*3*), a rise of temperature would also provoke a rise of (B_1/B_2) and in turn a smaller coverage at the transition. Therefore, it must be accepted that the surface is covered by an impurity coming from the residual atmosphere and this latter must be desorbed in order to make possible the adsorption of the reacting gases and in turn the detection of the transition. This hypothesis accounts well for the rising of the temperature limit when the pressure decreases. Indeed, the lower the working pressure, the larger the ratio between the partial pressure of the reacting gases. Measurements at lower residual pressure in a UHV vessel (residual pressure 10^3 lower) are planned.

c. Curve Parameter Calculations

Following the discussion above, it can be considered that in our working conditions, the system obeys an intermediate case

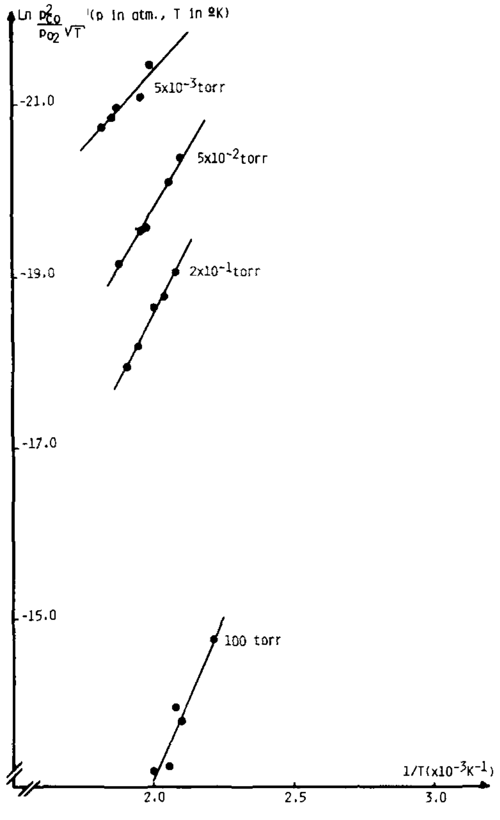

FIG. 6. Plot of the critical ln $p^2_{CO}/(p_{O_2}\sqrt{T})$ determined on epitaxial Pt(100) film versus $1/T$.

(zone C of Fig. 4). A direct estimation of the activation energies is then impossible.

Some of the Eq. (1) parameters can be approximated by proceeding as follows: when considering Eq. (6) and deriving ln (B_2/C) as a function of ln (B_1/B_2), it gives

$$\frac{d \ln (B_2/C)}{d \ln (B_1/B_2)} = \frac{-1}{X} = \frac{-1}{Y} = \frac{-2}{1 - (B_1/B_2)}. \quad (12)$$

Now deriving ln (B_2/C) and ln (B_1/B_2) as functions of $1/T$ and neglecting the $\sqrt{T}$, σ_{CO}, σ_{O_2}, and C' change with the temperature, we obtain

$$\frac{d \ln (B_2/C)}{d(1/T)} = C'' - B_2'' \quad (13)$$

$$\frac{d \ln (B_1/B_2)}{d(1/T)} = \frac{d \ln (p_{CO}/p_{O_2})}{d(1/T)} + B_2''. \quad (14)$$

Due to the narrow range of temperatures where the study is made, $d \ln(p_{CO}/p_{O_2})/d(1/T)$ can be approximated to the slope of our experimental curves (Fig. 2a) which is denoted as $A(p)$.

Finally, approximating the derivative of Eq. (12) to the ratio of the derivatives of Eqs. (13) and (14) gives

$$\frac{C'' - B_2''}{A(p) + B_2''} = -\frac{1}{X}. \quad (15)$$

Assuming that the case $B_2 \gg C$ is realized at atmospheric pressure (1), the $C'' + B_2''$ value is extrapolated from Fig. 3b. Postulating some values of B_2'', the quantities σ_{CO}/σ_{O_2}, B_2/C, and σ_{O_2}/C' are calculated (see Table 1).

These calculated parameters do not change considerably as a function of the chosen B_2'' values and are in good agreement with the values found by Sales *et al.* (9) despite the fact that this curve parameter calculation is based upon some assumptions: the invariance of C', σ_{O_2}, and σ_{CO} versus the total pressure and the invariance of the activation energies versus the surface coverage.

One of the main objections which can be made is the fact that CO desorption has been neglected. However, it is generally assumed that below 550°K, CO desorption has no appreciable effect (9). In such conditions, the model used here is quite similar to that of Turner *et al.* (11). In this work the $R \times (C'' + B_2'')$ value (17 kcal/mole) is very near our extrapolated one (16.2 kcal/mole).

In the work of Herz and Marin (10), diffusional effects are considered but they can be neglected here since the transition is detected from the inhibited phase to the active one (1). The only difference between the Herz and Marin models and the DDN model (7) is the coverage function appearing in Eq. (2). This latter becomes

$$\frac{dY}{dt} = B_2 \left(1 - X\frac{(1 - 2Y)}{(1 - Y)} - 2Y\right)^2 - CXY \quad (16)$$

according to model I of Ref. (10) and

$$\frac{dY}{dt} = B_2 \left(1 - X\frac{(1 - 2Y)}{(1 - Y)} - 2Y\right)(1 - 2Y) - CXY \quad (17)$$

according to model II of Ref. (10).

The coverage function of atomic oxygen in these equations accounts for a maximum oxygen coverage of 0.5 suggested by some studies (12–14) but that does not necessarily account for the adsorption rate of oxygen at lower oxygen coverage. The simpler function $(1 - X - Y)^2$ can also be good and has the advantage of giving an analytical relationship between the critical point and the activation energies. Anyway at the transition, the coverages do not exceed 0.5 and moreover the critical ratios p_{CO}/p_{O_2} given by Herz and Marin are in good agreement with ours. It proves that the choice of more complicated coverage functions adds no relevant effects.

5. CONCLUSIONS

We have studied the transition between two stationary states of carbon monoxide oxidation on platinum in a large range of pressures. Two types of platinum films have been used, namely, polycrystalline Pt deposited on oxidized silicon wafers and epitaxial Pt(100) evaporated on LiF(100). The transition has been detected by using a Kelvin probe.

The critical [CO]/[O_2] ratio corresponding to the transition has been found to be greater than at atmospheric pressure (*1*). This is in good agreement with the results obtained in UHV (*4, 5*).

On polycrystalline Pt films, our study was considerably limited by the fact that this type of sample recrystallizes during the measurements. This is not the case for epitaxial Pt films.

The logarithm of the critical [CO]/[O_2] ratio has been plotted versus $1/T$ for the different working pressures. Using the DDN model (*7*) some kinetic parameters have been calculated and are found to be in good agreement with the literature.

Some results suggest that the catalyst surface may be contaminated by an impurity present in the residual atmosphere. Measurements in a UHV vessel are planned in order to avoid this problem.

REFERENCES

1. Dauchot, J. P., and Dath, J.-P., *J. Catal.* **86,** 373 (1984).

2. Dauchot, J. P., and Van Cakenberghe, J., *Nature* **246,** No. 152, 61 (1973).

3. Engel, T., and Ertl, G., *in* "Advances in Catalysis," Vol. 28, p. 1 Academic Press, New York, 1979.

4. Golchet, A., and White, J. M., *J. Catal.* **53,** 266 (1978).

5. Matsushima, T., Almy, D. B., and White, J. M., *Surf. Sci.* **67,** 89 (1977).

6. Winterbottom, W. L., *Surf. Sci.* **36,** 205 (1973).

7. Dagonnier, R., Dumont, M., and Nuyts, J., *J. Catal.* **66,** 130 (1980).

8. Dagonnier, R., and Nuyts, J., *J. Chem. Phys.* **2061,** 65 (1976).

9. Sales, B. C., Turner, J. E., and Maple, M. B., *Surf. Sci.* **114,** 381 (1982).

10. Herz, R. K., and Marin, S. P., *J. Catal.* **65,** 281 (1980).

11. Turner, J. E., Sales, B. C., and Maple, M. B., *Surf. Sci.* **103,** 54 (1981).

12. McCabe, R. W., and Schmidt, L. D., *Surf. Sci.* **66,** 101 (1977).

13. Conrad, H., Ertl, G., and Kuppers, J., *Surf. Sci.* **76,** 323 (1978).

14. Fisher, G. B., Sexton, B. A., and Gland, J. L., *J. Vac. Sci. Technol.* **17,** 144 (1980).